Alfarama Journal of Basic & Applied Sciences

Faculty of Science Port Said University

https://ajbas.journals.ekb.eg
ajbas@sci.psu.edu.eg

http://sci.psu.edu.eg/en/

October 2024, Volume 5, Issue IV (Special Issue)

DOI:**https://doi.org/10.21608/AJBAS.2024.315398.1227**

ISSN 2682-275X

Submitted: 26/08/2024

Accepted: 16/09/2024

Pages: 549 - 560

Biogenic Hydroxyapatite from Bovine Bone: Synthesis, Multi-technique Characterization, and Its Potential in Dye Removal

I.M. Serag[1,*], A.M. Abdelghany[2], F.I. El-Dossoki [1]

[1] Chemistry Department, Faculty of Science, Port Said University, Port Said *42526*, Egypt.
[2] Spectroscopy Department, Physics Division, National Research Centre, Dokki 12311, Giza, Egypt.

*** Correspondence author:** islam.serag2022@gmail.com

ABSTRACT

This study explores the synthesis of biogenic hydroxyapatite (HA) from bovine bone and its application in methylene blue (MB) dye removal from wastewater. The HA was synthesized through a multi-step process involving cleaning, defatting, and calcination of bovine bones at 900°C for 6 hours. The resulting material was characterized using X-ray diffraction (XRD), and Fourier Transform Infrared spectroscopy (FTIR). The XRD and FTIR analyses confirmed the successful synthesis of high-purity, well-crystallized hydroxyapatite. Batch adsorption studies were conducted to evaluate the HA's efficiency in removing MB from aqueous solutions. The effects of various parameters, including pH, adsorbent dose, contact time, ionic strength, and temperature, were investigated. The results showed optimal MB removal at pH 11.0, with a 3 g/L adsorbent dose and a 20-minute contact time. The adsorption process was found to be exothermic, with efficiency decreasing at higher temperatures. Adsorption isotherms were analyzed using Langmuir and Freundlich models, with the Freundlich model providing a better fit to the experimental data. This study demonstrates the potential of bovine bone-derived HA as an effective and sustainable adsorbent for dye removal in wastewater treatment applications.

Key Words: Hydroxyapatite; bovine bone; water treatment; methylene blue; adsorption.

1. INTRODUCTION

Hydroxyapatite (HA), a calcium phosphate ceramic with the chemical formula $Ca_{10}(PO_4)6(OH)_2$, is a crucial biomaterial due to the main inorganic constituent of human bone and teeth [1-3]. Its synthesis has been extensively studied using various methods and sources, each offering unique advantages and challenges. Synthetic routes include wet chemical precipitation [4], sol-gel processing [5], hydrothermal methods [6], and solid-state reactions [7]. These techniques allow for precise control over stoichiometry, crystallinity, and particle morphology, but often involve complex procedures or high-temperature processing.

In contrast, biological sources offer a more sustainable and potentially cost-effective approach to HA production. Marine sources such as fish bones, coral, and seashells have been explored, yielding HA with varying properties depending on the species and extraction method [8, 9]. Plant-based sources, including fruit peels and wood, have also been investigated, though these typically require more extensive processing to remove organic components [10, 11].

Among biological sources, bovine bone has emerged as a remarkably promising raw material for HA synthesis [12, 13]. This method is advantageous due to the high availability of bovine bone as a by-product of the meat industry and its close compositional similarity to human bone. HA derived from bovine bone often retains trace elements present in natural bone, which can enhance its biological performance [14]. The calcination temperature significantly influences the properties of the resulting HA, affecting crystallinity, phase composition, and particle size. Lower temperatures (around 600-800°C) tend to preserve more of the natural bone structure and may retain some carbonate content, resulting in carbonated HA which more closely mimics natural bone mineral minerals. Higher temperatures (above 1000°C) produce more crystalline HA but may lead to the formation of other calcium phosphate phases [15, 16]. The properties of bovine bone-derived HA, including its crystallinity, particle size, surface area, and trace element composition, can be tailored by adjusting processing parameters. This versatility makes it suitable for various biomedical applications, including bone grafts, dental implants, and drug delivery systems.

Hydroxyapatite (HA) has emerged as a promising material for environmental remediation, particularly in the removal of heavy metals and dyes from wastewater [17]. Its excellent adsorption properties, high surface area, low water solubility, high stability, and biocompatibility make it an ideal candidate for water treatment applications. HA's effectiveness in heavy metal removal stems from its ability to undergo ion exchange, surface complexation, and dissolution-precipitation reactions. The calcium ions in HA can be readily exchanged with various heavy metal ions such as lead, cadmium, copper, and zinc, effectively immobilizing these contaminants [18]. Additionally, the phosphate and hydroxyl groups on HA's surface can form stable complexes with metal ions, further enhancing its removal capacity. For dye removal, HA demonstrates high adsorption efficiency due to its porous structure and large specific surface area. The interaction between HA and dye molecules involves electrostatic attractions, hydrogen bonding, and π-π interactions, depending on the dye's chemical structure [19, 20]. HA's performance in contaminant removal can be further improved through various modification techniques, such as doping with other elements, creating composites with other materials, or adjusting its morphology and particle size. These modifications can enhance HA's adsorption capacity, selectivity, and recyclability. Moreover, HA's biocompatibility and non-toxicity make it an environmentally friendly option compared to conventional adsorbents [20, 21].

Hydroxyapatite (HA) from natural sources offers several benefits for removing methylene blue dye from aqueous media. Its high surface area and porous structure provide excellent adsorption capacity for the dye molecules. Natural HA, derived from sources like fish bones or eggshells, is cost-effective and environmentally friendly compared to synthetic alternatives. HA's stable chemical structure allows it to function effectively across various pH levels and temperatures. Its biocompatibility and non-toxicity make it safe for water treatment applications. Additionally, HA can be modified or combined with other materials to enhance its dye removal efficiency. The calcium and phosphate ions in HA may also interact with the dye molecules, further aiding in their removal. These advantages make natural hydroxyapatite an attractive option for sustainable and efficient methylene blue removal from aqueous solutions.

Ongoing research focuses on addressing and exploring novel applications of optimized HA from bovine bone as a natural source in methylene blue (MB) dye removal from wastewater as water scarcity and pollution continue to be global concerns. Such removal represents a promising avenue for sustainable water management and environmental protection.

2. MATERIALS AND METHODS

2.1 Materials used: Bovine bone is supplied by the national market, ethyl alcohol is supplied by Elnasr Pharmaceutical Chemicals Co., distilled water, Methylene blue dye (MB) supplied by Sigma Aldrich Co.

2.2 Synthesis of hydroxyapatite (HA): The preparation of hydroxyapatite (HA) from bovine bone is a multi-step process that begins with the thorough cleaning and defatting of the raw bone material. Initially,

the bones are mechanically cleaned to remove any adherent soft tissues, tendons, and ligaments. They are then cut into smaller pieces to increase surface area for subsequent treatments. The bone fragments undergo defatting, typically using a combination of hot water and organic solvents (ethyl alcohol). This process removes lipids, marrow, and other organic impurities. Following defatting, the bones are thoroughly rinsed with distilled water and dried. The next crucial step is the calcination process to remove any organic component residuals. This process is carried out in a high-temperature furnace, with temperatures typically ranging from 900°C, held for 6 hours. During calcination, all organic materials, including collagen and other proteins, are combusted and removed, leaving behind the inorganic HA structure. This step also eliminates potential pathogens, ensuring the safety of the final product. After calcination, the bone material, now primarily composed of HA, often undergoes a milling process to achieve the desired particle size using planetary milling adopting different-sized zirconium balls at 5000 rpm for 3 hours.

2.3 Sample Characterization: X-ray spectroscopy technique (Brucker Axs-D8 Advance, utilizing a CuKα radiation source) is utilized to determine the crystal structure of studied samples adopting X-ray radiation with a λCuKα = 0.1540 nm in the range of 3 to 70̊ angle. ATR-FTIR was measured using Bruker VERTEX 80 (Germany) combined Platinum Diamond ATR, which comprises a diamond disk as that of an internal reflector was used in the range 4000–400 cm^{-1} with resolution 4 cm^{-1}. The surface topography of the produced sample was examined using a scanning electron microscope type QUANTA FEG 250 FE-SEM supplemented with an EDX unit operating at 20 kV accelerating voltage. The pH was measured by a Metrohm 632 digital pH meter (Metrohm Autolab, Herisau, Switzerland). The concentration of MB was determined using 7300 Genway spectrophotometer (Cole-Parmer Ltd., Staffordshire, UK).

2.4 Batch adsorption study: Batch adsorption tests were performed by shaking flasks containing a definite amount of HA (V) added to a given volume (V) of MB solution of concentration C_i at a certain pH. After a time, the solid phase was settled by centrifugation and the concentration of MB in the filtrate (C_f) was determined by spectrophotometry at 665 nm. The removal efficiency (R) of the dye and the adsorption capacity (q_e) were determined from Eq. (1) and Eq. (2), respectively [22-24].

$$R\% = \frac{C_i - C_f}{C_i} \times 100 \quad (1)$$

$$q_e\ (mg\ g^{-1}) = \frac{(C_i - C_e)\,V}{m} \quad (2)$$

The optimization was carried out by a one-at-a-time approach. The initial pH of the working solutions was investigated in the range of 2.0 – 12.0 and adjusted using NaOH and HCl solutions. The impact of adsorbent doses ranging from 0.5 to 10.0 g L^{-1} was examined. The effect of shaking time was explored by altering the shaking times from 5.0 to 60.0 min for a fixed initial dye concentration of 100 mg L^{-1} with 10.0 mg of HA in a 50 mL solution. Other parameters were investigated as previously reported works [22].

The point of zero charge (PZC) in adsorption experiments refers to the pH at which the surface of an adsorbent material has a net electrical charge of zero. At this specific pH, the adsorbent's surface contains an equal number of positive and negative charges, resulting in electrical neutrality. PZC is a critical parameter in adsorption studies because it significantly influences the interaction between the adsorbent and charged species in solution. When the solution pH is below the PZC, the adsorbent surface becomes positively charged, favoring the adsorption of anions. Conversely, when the pH is above the PZC, the surface acquires a negative charge, promoting the adsorption of cations. Understanding the PZC of an

adsorbent material allows to predict and optimize adsorption processes by manipulating the solution pH relative to the adsorbent's PZC, thereby enhancing the removal efficiency of target pollutants such as dyes or heavy metals from aqueous media.

3. RESULTS AND DISCUSSION

3.1. HA Characterization

Figure (1) reveals X-ray diffraction pattern (XRD) of the studied hydroxyapatite powder (HA).The X-ray diffraction pattern (XRD) analysis of the studied sample revealed a pattern in complete agreement with the standard reference pattern of hydroxyapatite [$Ca_{10}(PO_4)_6(OH)_2$], as previously reported with a card no. 01-085-3476 from the International Centre for Diffraction Data (ICDD) database. This strong correlation is evidenced by the precise alignment of all major diffraction peaks in terms of both position and relative intensity. The most prominent peaks and their corresponding Miller indices are as follows: The strongest peak, observed at approximately $2\theta = 31.8°$, is indexed as the (211) reflection. This is closely followed by the (112) peak at around 32.2°. Other significant peaks include the (300) reflection at about 32.9°, the (202) at 34.0°, and the (310) at 39.8°. The characteristic (002) peak, indicative of the c-axis orientation in the crystal structure, is typically observed at around 25.9°. Additional important reflections include the (222) at approximately 46.7°, the (213) at 49.5°, and the (004) at 53.1°. The presence and relative intensities of these peaks, along with their precise positions, are crucial for confirming the phase purity and crystallinity of the hydroxyapatite sample [25, 26].

The absence of any additional peaks in the diffraction pattern indicates the sample's high purity, free from crystalline impurities or secondary phases. The observed peak sharpness suggests good crystallinity, comparable to well-formed hydroxyapatite crystals. Furthermore, the low and smooth background of the XRD pattern further confirms the sample's high purity and crystallinity. These findings collectively demonstrate the successful synthesis of high-purity, well-crystallized hydroxyapatite in our sample.

Figure (2) reveals the FTIR spectral absorption data of the studied synthesized HA. The Fourier Transform Infrared (FTIR) spectroscopy analysis of the synthesized hydroxyapatite [$Ca_{10}(PO_4)_6(OH)_2$] reveals a characteristic absorption spectrum that confirms its structural composition. The spectrum exhibits several distinctive peaks and features that are indicative of the various chemical bonds and functional groups present in the hydroxyapatite structure. A small peak observed at 1420 cm^{-1} can be attributed to the carbonate (CO_3^{2-}) substitution in the apatite structure, suggesting minor carbonate incorporation during synthesis. The spectrum shows prominent shoulders at 1090 and 960 cm^{-1}, which are associated with the asymmetric (ν_3) and symmetric (ν_1) stretching modes of the phosphate (PO_4^{3-}) groups, respectively. The most intense and sharp peak at 1025 cm-1 is characteristic of the triply degenerate asymmetric (ν_3) stretching vibration of the PO_4^{3-} groups, further confirming the presence of phosphate in the hydroxyapatite structure. Less intense peaks observed at 630 and 600 cm-1 can be assigned to the hydroxyl (OH^-) libration mode and the (ν_4) bending mode of PO_4^{3-}, respectively. The peak at 565 cm-1 is attributed to the (ν_4) O-P-O bending mode of the phosphate groups. Two additional small peaks at 470 and 420 cm-1 are likely associated with the (ν2) O-P-O bending modes of the phosphate tetrahedra [26-28]. The presence and relative intensities of these peaks, particularly the strong phosphate and hydroxyl vibrations, provide strong evidence for the successful synthesis of hydroxyapatite. The minor carbonate peak suggests a slight B-type substitution, where carbonate ions replace some phosphate groups in the crystal lattice. Overall, this FTIR spectral data comprehensively supports the formation of hydroxyapatite with its characteristic functional groups and offers insights into its structural composition.

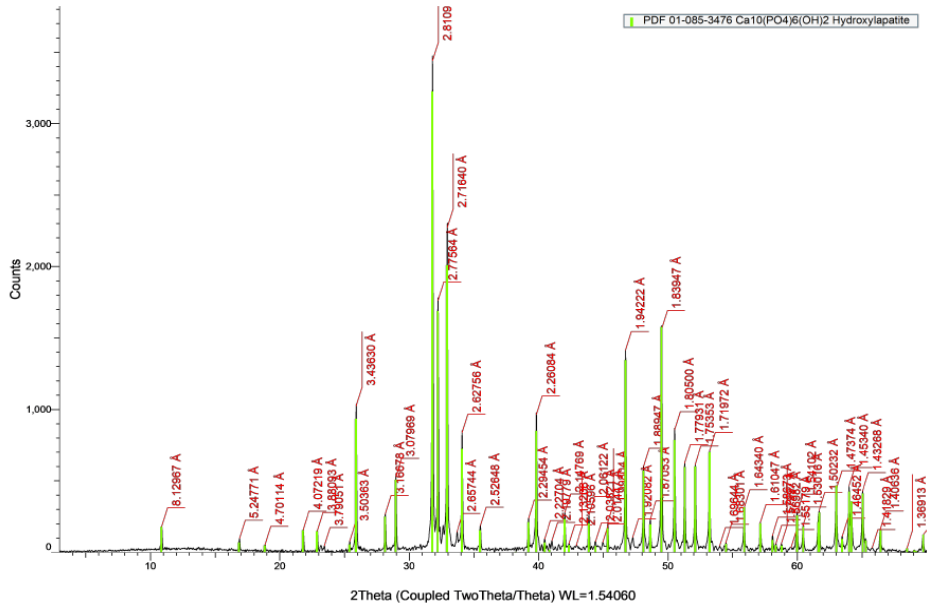

Fig.1 XRD pattern of the studied synthesized HA.

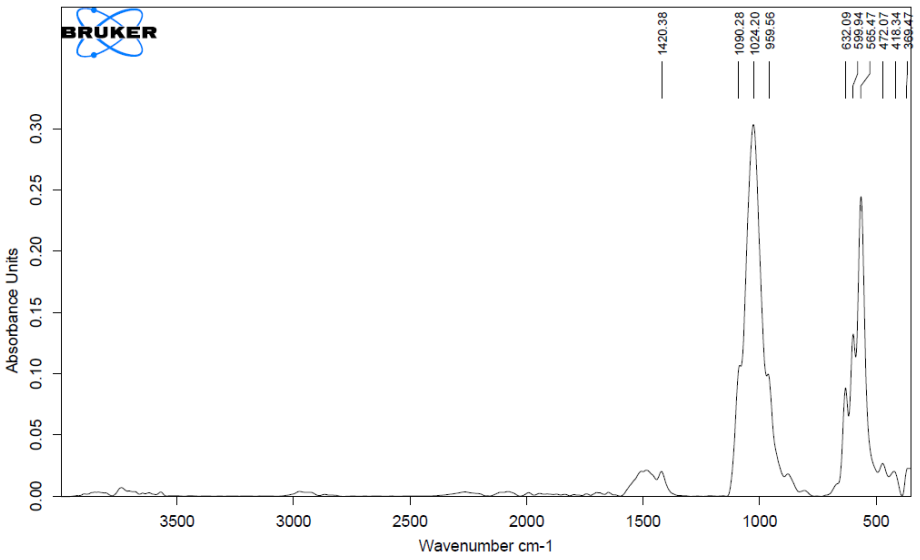

Fig.2 FTIR Spectral absorption data of the studied synthesized HA

3.2. Adsorption studies

3.2.1. Effect of pH: The influence of initial solution pH on methylene blue (MB) removal by hydroxyapatite (HA) was investigated under specific experimental conditions. The study revealed a gradual increase in MB removal efficiency as pH increased, reaching a maximum of 99.5% at pH 11.0 and above. This phenomenon can be explained by the point of zero charge (pHPZC) of HA shown in fig.3, determined to be 8.0. At pH values above the pHPZC, HA's surface becomes negatively charged, enhancing the adsorption of cationic MB molecules through electrostatic attraction. Conversely, at pH levels below the pHPZC, HA's surface acquires a positive charge, resulting in electrostatic repulsion between the surface and cationic MB molecules, thereby reducing adsorption efficiency. This pH-dependent behavior highlights the critical role of electrostatic interactions in the adsorption process [29]. The findings suggest that alkaline conditions significantly favor MB removal by HA, with optimal

performance observed at pH 11.0 and higher. This understanding of pH effects on MB adsorption by HA provides valuable insights for optimizing dye removal processes in wastewater treatment applications, emphasizing the importance of pH control in achieving maximum adsorption efficiency.

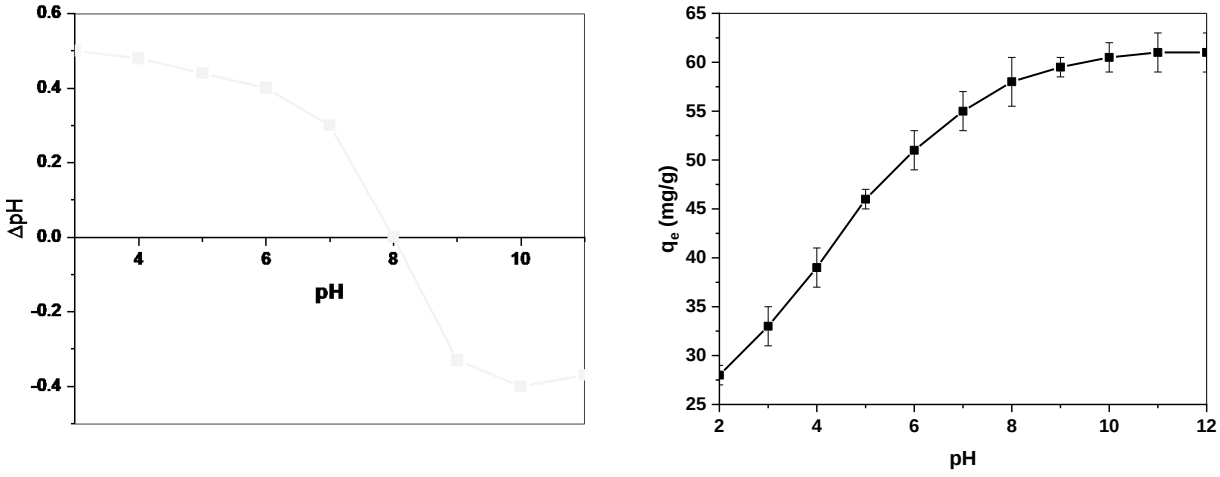

(a) **(b)**

Fig.3 (a) pH_{PZC} of HA , (b) Effect of pH on the uptake of MB by HA

3.2.2. Effect of HA dose: The removal of MB by HA was investigated using specific experimental parameters, including a 20 mg/L MB concentration, pH 11.0, 20 min shaking time, 25°C temperature, and varying HA concentrations (0.5-10.0 g/L). Fig. 4 demonstrates that MB removal efficiency increases with HA amount, reaching maximum performance at 3 g/L. As HA concentration increased from 0.5 to 6 g/L, dye removal improved from 44% to 91%, attributed to increased surface area and active centers. Based on these results, a sorbent dose of 3 g/L was selected for subsequent experiments.

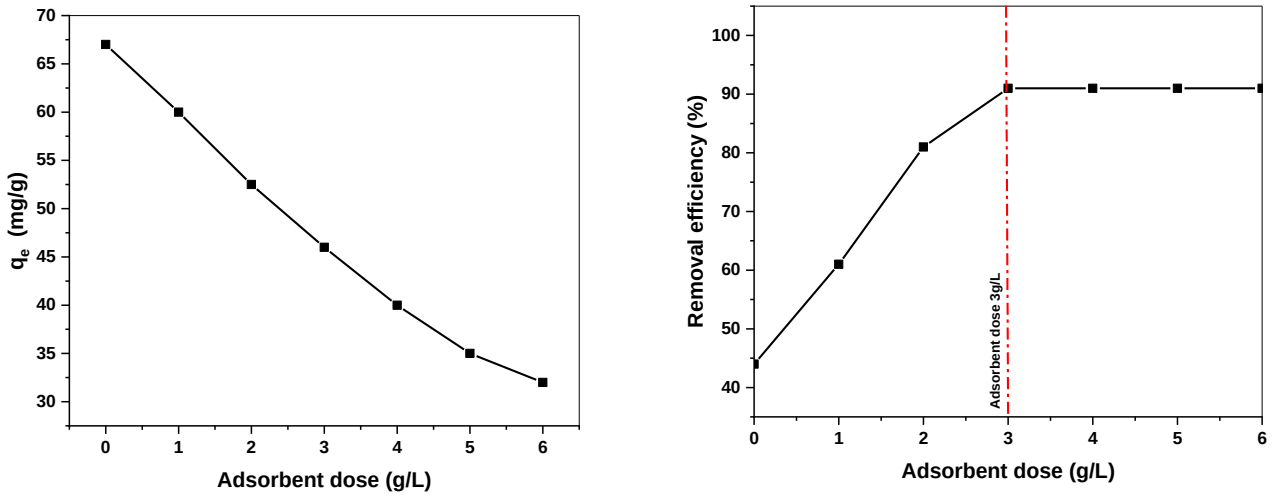

(a) **(b)**

Fig.4 Effect of sorbent dose on the removal of MB by HA.

3.2.3. Effect of shaking time: The impact of shaking time on MB adsorption by HA is shown in Fig. 5. A significant 60.2% removal occurs within the first 5 minutes, with equilibrium reached after 20 minutes. The initial rapid adsorption rate can be attributed to the abundance of available active sites and a high MB concentration gradient. As the process continues, the adsorption rate slows due to fewer unoccupied

active sites and a reduced dye concentration gradient. Based on these results, a 20-minute shaking time was determined to be optimal for the process.

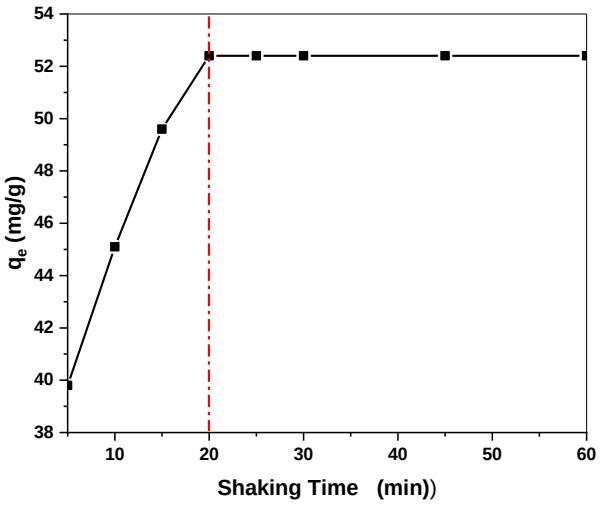

Fig. 5 Effect of shaking time on the removal of MB by HA

3.2.4. Effect of ionic strength: The impact of ionic strength on the absorption of MB by HA was investigated by varying the concentration of NaCl from 0.1 to 5.0% (w/v). As previously found, increasing ionic strength resulted in a reduction in MB removal (Fig. 6). The presence of a strong electrolyte such as NaCl in the medium may decrease the electrostatic interaction between opposing charges at the sorbent surface and on dye molecules, resulting in a decrease in adsorbed capacity as NaCl concentration increases, that is termed salting out effect [31].

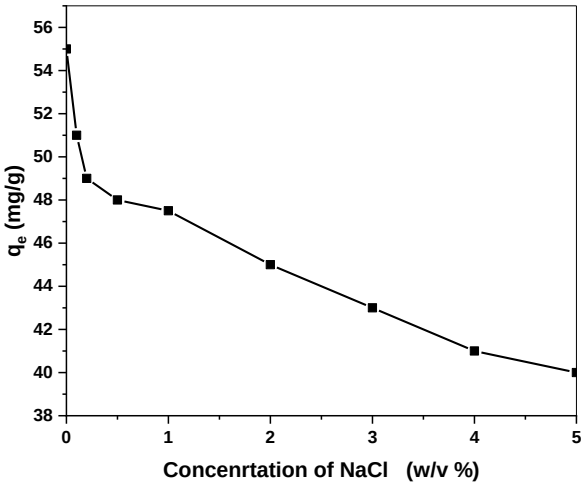

Fig.6 Effect of NaCl concentration of the removal of MB by HA

3.2.5. Effect of temperature: The influence of temperature on MB removal by HA was examined through batch adsorption experiments conducted between 25° and 60°C. As shown in Fig. 7, MB removal efficiency decreases with increasing temperature, suggesting an exothermic adsorption process. This trend may be explained by the enhanced stability of positively charged MB molecules at lower temperatures, which promotes stronger electrostatic interactions with HA's active sites. Based on these findings, subsequent experiments were performed at room temperature (25°C).

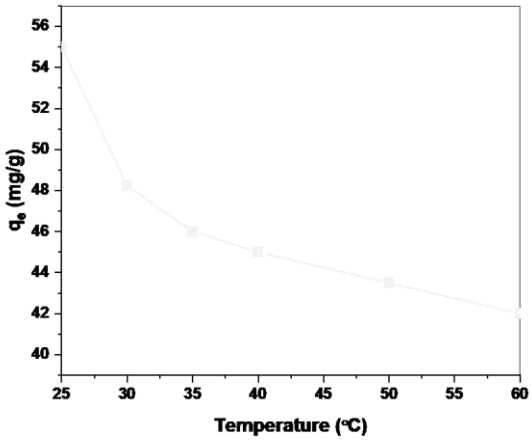

Fig. 7 Effect of temperature on the removal of MB by HA

3.3. Adsorption isotherm

Adsorption isotherms are mathematical models that describe the distribution of adsorbate molecules between the liquid and solid phases at equilibrium. These models are crucial for understanding the adsorption mechanism, surface properties, and affinity of the adsorbent. Two of the most commonly used adsorption isotherm models are the Langmuir and Freundlich isotherms.

The Langmuir isotherm assumes monolayer adsorption on a homogeneous surface with a finite number of identical sites. It suggests that adsorption occurs at specific sites on the adsorbent surface, and once a site is filled, no further adsorption can occur at that site. The Langmuir equation provides information about the maximum adsorption capacity and the energy of adsorption [32].

In contrast, the Freundlich isotherm is an empirical model that can be applied to multilayer adsorption on heterogeneous surfaces. It assumes that the adsorption energy decreases exponentially as the surface coverage increases. The Freundlich equation describes the non-ideal and reversible adsorption process and is not limited to monolayer formation [33].

Both models have their strengths and limitations, and the choice between them depends on the specific adsorbent-adsorbate system and experimental conditions. Researchers often apply both models to their data to determine which one provides a better fit and to gain insights into the adsorption mechanism.

The effect of MB initial concentration on the adsorption process was studied within the range of 5.0-350.0 mg /L as shown in Fig.8 at which a linear relationship between rate of dye adsorption and the dye concentrations within the range 20-250 mg/L and saturation behavior after 300 mg/L without no effect of adsorption process. The rapidly linear uptake of dye at lower concentrations attributed to the higher number of available active sites combined with and lower number of dye molecules. Further increase in MB dye concentration may results in a gradual decrease in dye adsorption process resulting from the possible saturation of the available active sites.

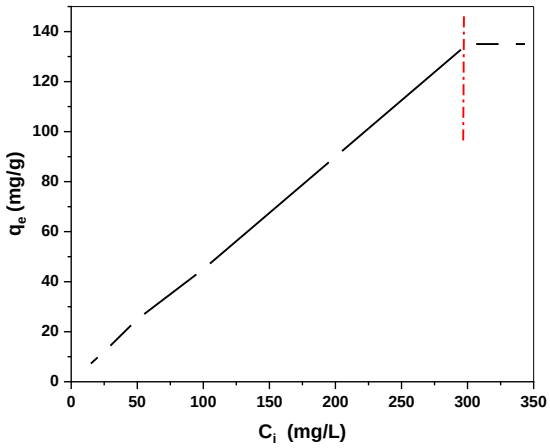

Fig. 8 effect of initial concentration for adsorption of MB on HA

Applying the linear equation for the Langmuir isotherm model [$C_e/q_e = C_e/q_{max} + 1/K_L\ q_{max}$] where C_e is the equilibrium concentration, q_{max} is the maximum sorption capacity (mg/L), K_L is the Langmuir isotherm constant related to free energy of sorption process. Ploting C_e/q_e against C_e (Fig. 9) yield a straight line fit with Langmuir isotherm model while Langmuir isotherm constant and q_{max} calculated from intercept and slope of the linear regression and observed in table (1). Moreover, the favorability of the adsorption process can be evaluated by calculating the Langmuir isotherm equilibrium parameter $R_L=1/\ K_L\ C_i$ which must lie between 0 and 1. Therfore R_L =1.054 means that the isotherm is defined as unfavorable.

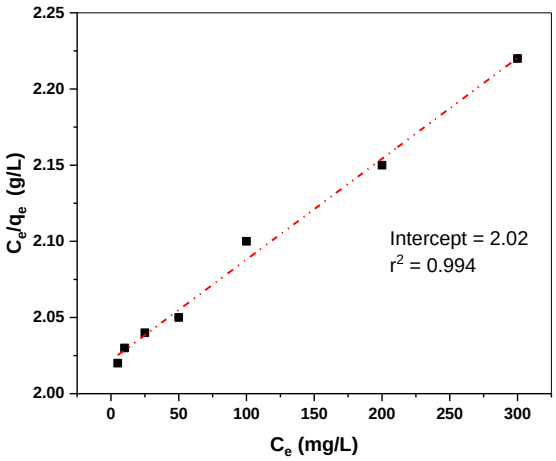

Fig. 9 Langmuir isotherm plot for adsorption of MB on HA

The Freundlich isotherm model equation [log q_e = log K_f + 1/ n log C_e], where 1/n and K_f are Freundlich isotherm constants obtained through potting log q_e against log C_e linear plot was obtained as shown in Fig.10 with a slope of 1/n (1.02) (more than unity) which refers to a heterogeneous surface with maximum interactions between the adsorbed ions and K_f was calculated from the intercept which indicates the quantity of the M.B adsorbed on the surface of HA.

The linear relation obtained shows high fitting of the adsorption results with a high determination coefficient (R2 = 0.999).

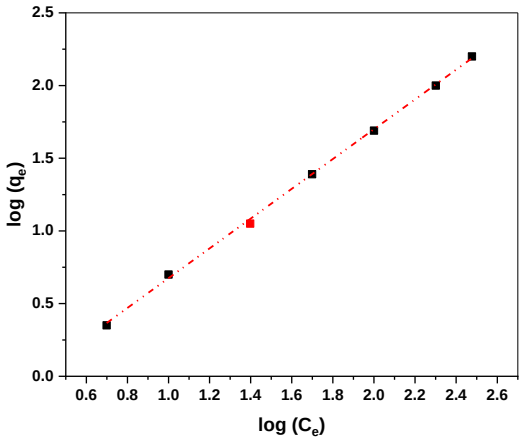

Fig.10 Freundlich isotherm plot for adsorption of MB on HA

Table. 1 Adsorption isotherm parameters of M.B on sugarcane

Isotherm model	Parameter	Values	R^2
Langmuir	q_{max}	151.7	0.994
	K_L	0.0032	
	R_L	1.054	
Freundlich	n/1	1.02	0.999
	K_f	2.26	

4. CONCLUSION

In conclusion, this study successfully demonstrates the synthesis of high-quality hydroxyapatite from bovine bone and its effective application in methylene blue dye removal from aqueous solutions. The XRD and FTIR analyses confirmed the production of pure, crystalline HA, highlighting the efficacy of the synthesis method. The adsorption studies revealed that the HA-based adsorbent performs optimally under alkaline conditions (pH 11.0), with a relatively low adsorbent dose (3 g/L) and short contact time (20 minutes). These findings suggest that bovine bone-derived HA could be a cost-effective and environmentally friendly alternative for wastewater treatment. The adsorption process was found to be exothermic, indicating better performance at room temperature. The Freundlich isotherm model provided the best fit for the adsorption data, suggesting a heterogeneous adsorption surface with multilayer coverage. The high adsorption capacity and favorable adsorption characteristics of the synthesized HA underscore its potential as a sustainable solution for dye removal in industrial wastewater treatment. Future research could focus on scaling up the process, investigating the adsorbent's regeneration capabilities, and exploring its effectiveness in removing other types of pollutants.

5. REFERENCES

[1] V. P. Orlovskii, V. S. Komlev, and S. M. Barinov, " Hydroxyapatite and hydroxyapatite-based ceramics", Inorganic materials, 38, 973-984, 2002.

[2] A. K. Nayak, "Hydroxyapatite synthesis methodologies: an overview", International Journal of ChemTech Research, 2(2), 903-907, 2010.

[3] K. P. Sanosh, M. C. Chu, A. Balakrishnan, Y. J. Lee, T. N. Kim, and S. J. Cho, "Synthesis of nano hydroxyapatite powder that simulate teeth particle morphology and composition", *Current Applied Physics*, *9*(6), 1459-1462, 2009.

[4] N. Monmaturapoj, "Nano-size hydroxyapatite powders preparation by wet-chemical precipitation route", *Journal of Metals, Materials and Minerals*, *18*(1), 15-20, 2008.

[5] K. P. Sanosh, , M. C. Chu, A. Balakrishnan, T. N. Kim, and S. J. Cho, "Preparation and characterization of nano-hydroxyapatite powder using sol-gel technique", *Bulletin of Materials Science*, *32*, 465-470, 2009.

[6] N. M. Pu'ad, R. A. Haq, H. M. Noh, H. Z. Abdullah, M. I. Idris, and T. C. Lee, "Synthesis method of hydroxyapatite: A review", *Materials Today: Proceedings*, *29*, 233-239, 2020.

[7] H. R. Javadinejad, and R. Ebrahimi-Kahrizsangi,"Thermal and kinetic study of hydroxyapatite formation by solid-state reaction", *International Journal of Chemical Kinetics*, *53*(5), 583-595, 2021.

[8] T. Laonapakul,"Synthesis of hydroxyapatite from biogenic wastes", *Engineering and Applied Science Research*, *42*(3), 269-275, 2015.

[9] G. Borciani, T. Fischetti, G. Ciapetti, M. Montesissa, N. Baldini, and G. Graziani, "Marine biological waste as a source of hydroxyapatite for bone tissue engineering applications", *Ceramics International*, *49*(2), 1572-1584, 2023.

[10] M. Manoj, and A. Yuan" A plant-mediated synthesis of nanostructured hydroxyapatite for biomedical applications: a review", *RSC advances*, *10*(67), 40923-40939, 2020.

[11] R. Veluswamy, G. Balasubramaniam, M. Natarajan, M. Krishnaswamy, B. A. Chinnappan, S. Nagarajan, and D. Velauthapillai," Multifunctional and sustainable hydroxyapatite from natural products for biomedical and industrial applications-A comprehensive review", *Sustainable Chemistry and Pharmacy*, *41*, 101653, 2024.

[12] C. Y. Ooi, M. Hamdi, and S. Ramesh, "Properties of hydroxyapatite produced by annealing of bovine bone", *Ceramics international*, *33*(7), 1171-1177, 2007.

[13] A. Ruksudjarit, K. Pengpat, G. Rujijanagul, and T. Tunkasiri, "Synthesis and characterization of nanocrystalline hydroxyapatite from natural bovine bone", *Current applied physics*, *8*(3-4), 270-272, 2008.

[14] A. Moradi, M. Pakizeh, and T. Ghassemi, "A review on bovine hydroxyapatite; extraction and characterization", *Biomedical Physics & Engineering Express*, *8*(1), 012001, 2021.

[15] M. K. Herliansyah, M. Hamdi, A. Ide-Ektessabi, M. W. Wildan, and J. A. Toque, "The influence of sintering temperature on the properties of compacted bovine hydroxyapatite", *Materials Science and Engineering, C*, *29*(5), 1674-1680, 2009.

[16] A. M. Castillo-Paz, M. Gomez-Resendiz, D. F. Cañon-Davila, B. A. Correa-Piña, R. Ramírez-Bon, and M. E. Rodriguez-Garcia, "The effect of temperature on the physical-chemical properties of bovine hydroxyapatite biomimetic scaffolds for bone tissue engineering", *Ceramics international*, *49*(21), 33735-33747, 2023.

[17] R. Verma, S. R. Mishra, V. Gadore, and M. Ahmaruzzaman,"Hydroxyapatite-based composites: excellent materials for environmental remediation and biomedical applications", *Advances in Colloid and Interface Science*, *315*, 102890, 2023.

[18] A. Nayak, and B. Bhushan "Hydroxyapatite as an advanced adsorbent for removal of heavy metal ions from water: Focus on its applications and limitations", *Materials Today: Proceedings*, *46*, 11029-11034, 2021.

[19] S. Pai, M. S. Kini, and R. Selvaraj, "A review on adsorptive removal of dyes from wastewater by hydroxyapatite nanocomposites", *Environmental Science and Pollution Research*, *28*(10), 11835-11849, 2021.

[20] A. A. El-Zahhar, and N. S. Awwad, "Removal of malachite green dye from aqueous solutions using organically modified hydroxyapatite", *Journal of Environmental Chemical Engineering*, *4*(1), 633-638, 2016.

[21] H. Hou, R. Zhou, P. Wu, and L. Wu, "Removal of Congo red dye from aqueous solution with hydroxyapatite/chitosan composite", *Chemical engineering journal*, *211*, 336-342, 2012.

[22] W. I. Mortada, K. A. Nabieh, and A. M. Abdelghany, "Efficient and low-cost surfactant-assisted solid phase extraction procedure for removal of methylene blue using natural dolomite", *Water, Air, & Soil Pollution*, *234*(6), 363, 2023.

[23] M. I. El-Khaiary, and G. F. Malash, "Common data analysis errors in batch adsorption studies", *Hydrometallurgy*, *105*(3-4), 314-320, 2011.

[24] B. O. Isiuku, P. C. Okonkwo, and C. D. Emeagwara, "Batch adsorption isotherm models applied in single and multicomponent adsorption systems–a review", *Journal of Dispersion Science and Technology*, *42*(12), 1879-1897, 2021.

[25] A. Ślósarczyk, Z. Paszkiewicz, and C. Paluszkiewicz, "FTIR and XRD evaluation of carbonated hydroxyapatite powders synthesized by wet methods", *Journal of Molecular Structure*, *744*, 657-661, 2005.

[26] M. Mir, F. L. Leite, P. S. D. P. Herrmann Junior, F. L. Pissetti, A. M. Rossi, E. L. Moreira, and Y. P. Mascarenhas, "XRD, AFM, IR and TGA study of nanostructured hydroxyapatite", *Materials Research*, *15*, 622-627, 2012.

[27] M. S. Hossain, and S. Ahmed, "FTIR spectrum analysis to predict the crystalline and amorphous phases of hydroxyapatite: a comparison of vibrational motion to reflection", *RSC advances*, *13*(21), 14625-14630, 2023.

[28] F. Baldassarre, A. Altomare, E. Mesto, M. Lacalamita, B. Dida, A. Mele, and F. Capitelli, "Structural Characterization of Low-Sr-Doped Hydroxyapatite Obtained by Solid-State Synthesis", *Crystals*, *13*(1), 117, 2023.

[29] M. Kosmulski, "The pH dependent surface charging and points of zero charge. X. Update", *Advances in Colloid and Interface Science*, 102973, 2023.

[30] A. Imessaoudene, S. Cheikh, A. Hadadi, N. Hamri, J. C. Bollinger, A. Amrane, and L. Mouni, "Adsorption performance of zeolite for the removal of congo red dye: Factorial design experiments, kinetic, and equilibrium studies", *Separations*, *10*(1), 57, 2023.

[31] A. Amrutha, G. Jeppu, C. R. Girish, B. Prabhu, and K. Mayer, "Multi-component adsorption isotherms: review and modeling studies", *Environmental Processes*, *10*(2), 38, 2023.

[32] O. P. Murphy, M. Vashishtha, P. Palanisamy, and K. V. Kumar, "A review on the adsorption isotherms and design calculations for the optimization of adsorbent mass and contact time", *ACS omega*, *8*(20), 17407-17430, 2023.